Journal of Power Sources 342 (2017) 175–182

Contents lists available at ScienceDirect

Journal of Power Sources

journal homepage: www.elsevier.com/locate/jpowsour

Li metal coated with amorphous Li_3PO_4 via magnetron sputtering for stable and long-cycle life lithium metal batteries

Liping Wang [a], Qingji Wang [a], Weishang Jia [a], Shulin Chen [b], Peng Gao [b], Jingze Li [a, *]

[a] State Key Laboratory of Electronic Thin Films and Integrated Devices, University of Electronic Science and Technology of China, Chengdu 610054, China
[b] School of Physics, Peking University, Beijing 100871, China

HIGHLIGHTS

- Glassy Li_3PO_4 thin film is homogeneously deposited onto lithium metal foils.
- Li_3PO_4 thin film has an electronic conductivity of 1.4×10^{-10} S/cm.
- Li_3PO_4 thin film has an ionic conductivity of 2.8×10^{-8} S/cm.
- Li_3PO_4 coated lithium metal anodes have long cycle life performance.

GRAPHICAL ABSTRACT

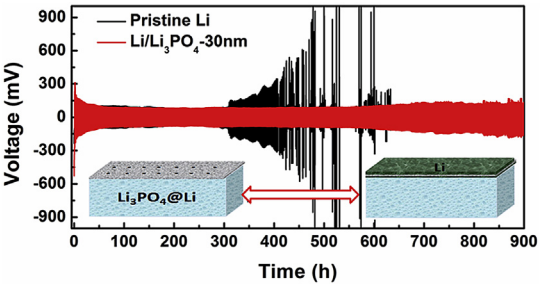

ARTICLE INFO

Article history:
Received 6 October 2016
Received in revised form
19 November 2016
Accepted 26 November 2016
Available online 21 December 2016

Keywords:
Amorphous
Lithium metal anode
Lithium phosphate
Lithium sulfur battery
Magnetron sputtering
Thin film

ABSTRACT

Lithium metal with high theoretical capacity (3860 mAh/g) and low operational voltage (−3.04 V vs. standard hydrogen electrode) reflects to be one of the most high energy density anodes for energy storage devices. While, its high chemical activity to continuously react with electrolytes causing low coulombic efficiency and formation of lithium dendrites leading safety concern limits practical applications. To conquer these challenges, amorphous Li_3PO_4 thin films with thickness of 0–200 nm are directly coated on the surface of Li metal foil via magnetron sputtering. The as-prepared Li_3PO_4 has almost insulated property with electronic conductivity of 1.4×10^{-10} S/cm and ionic conductivity of 2.8×10^{-8} S/cm. The conformal coating layer Li_3PO_4 can successfully suppress the lithium dendrites growth and improve its life span. The remarkable improvements of the Li_3PO_4-coated Li electrodes are mainly attributed to high chemical stability as well as amorphous nature of Li_3PO_4, which leads layer-by-layer growth Li film rather than islands form dendrites.

1. Introduction

Lithium metal anode is a contender in terms of energy density due to its high theoretical capacity (3860 mAh/g) and low operational voltage (−3.04 V vs. standard hydrogen storage) compared with Mg, Zn, Na metal ion anodes [1–6]. Moreover, the Li^+ stripped from lithium metal anodes has a smaller radius and monovalence, which can easily shuttle between cathodes and anodes under the conditions of preserving the framework structure with a small volume expansion/contraction [7,8]. However it has two challenges for the real applications. One is that metallic Li is too active (Gibbs energy −8.670 kJ/mol at room temperature) and hence it reacts with conventional organic liquid electrolytes to produce a solid electrolyte interface (SEI) layer, which is an ionic conductor and

* Corresponding author.
E-mail address: lijingze@uestc.edu.cn (J. Li).

http://dx.doi.org/10.1016/j.jpowsour.2016.11.097
0378-7753/

electronic insulator. The formed SEI, chemically unstable and unconformable, can be easily broken as a result of local stress during charge-discharge process leading exposure of fresh lithium which eventually brings in continuous consumption of both active Li metal and electrolyte. This finally causes low coulombic efficiency [9–11]. The other is the formation of lithium dendrites as a result of sluggish deposition of lithium ions that is correlated with the anionic mobility and electric field [12,13]. The formed lithium dendrite can puncture separators and lead to a short circuit with possible explosion due to the quickly accumulated heat [14–17].

Various attempts have been developed to circumvent these issues. In terms of stabilizing SEI layer, optimizing the electrolyte solvents and addition of additives with the aim of enlarging the electrochemical window in stability and modifying the SEI compositions have been shown to be effective ways [18,19]. Meanwhile, substitutions of the carbonate-based liquid electrolytes with solid state electrolytes are alternatives [20,21]. Moreover, artificial SEI layers via chemical or physical depositions onto the lithium metal before electrochemical activation are also practicable to improve the energy efficiency [22–25]. As for the prevention of lithium dendrites, tuning the local electric field via 3D current collectors to affect the initial nucleation of lithium deposition and improving thermal distribution through modify separators with a thermally conductive BN coating layer have been proved to be beneficial for lithium metal battery performance [14,26]. Simultaneously, lithium alloys (*i.e.* Li-Al, Li-B) are other important strategies to change lithium deposition morphology [27,28]. Thin layers, such as carbon films, PEDOT-co-PEG polymers, Al_2O_3 layers, and LiPON, directly coated on lithium metal foils have positive effects on safety and long cycle performance [25,29–32]. Zhang et al. employed amorphous carbon coatings on metallic Li foils by magnetron sputtering technique against the side reactions between Li electrode and electrolytes [23]. Recently, Li and coauthors reported that 200 nm thin film Li_3PO_4 generated by a chemical reaction with a high Young's Modulus 10–11 GPa can play roles to be an artificial ionic conducting SEI layer and to inhibit the lithium dendrite growth [22]. Wherever, it is still ambiguous and intriguing to know the intrinsic account of coating layers for the improvements. Since Bate et al. found that the polycrystalline Li_3PO_4 synthesized by chemical reactions has an ionic conductivity 10^{-18} S/cm, which is actually an ionic insulator [33]. In the case of lithium deposition/dissolution, lithium ions are accordingly difficult to pass through thick Li_3PO_4 films under high current rates (larger than 0.5 mA/cm^2 in normal cases). It is known that good chemical stability is prerequisite. While, there are limited references regarding the effect of transport properties, thickness, crystalline of these coating layers on the performance and the morphology evolutions of lithium metal. More importantly, the lithium electrochemical plate is a diffusion-limited process in which current density, electric field, and interfacial properties drive its growth modes (*i.e.* islands mode or layer-by-layer mode) [34,35]. Thus, the contribution of coating layer including of surface properties and morphologies on the early stage nucleation of lithium film should be paid special attentions.

In this study, herein, we fabricate amorphous Li_3PO_4 thin films with different thickness via magnetron sputtering onto the lithium foils to evaluate its impact on the electrochemical performance of lithium. Magnetron sputtering technique provides a facile and economic way to obtain homogeneous and compact films with thickness control via tuning sputtering time. Moreover, thin films obtained via magnetron sputtering at room temperature normally present glassy amorphous phases with the advantages of less grain boundaries, high ionic conductivity, and low surface energy as well as isotropy nature. As for the Li_3PO_4, it is more chemically stable than the well known lithium ion conductor LiPON, which is highly sensitive to air and moisture. It is found that the obtained Li_3PO_4 thin film, an almost insulate material, has an ionic conductivity of 10^{-8} S/cm and electronic conductivity of 10^{-10} S/cm. Lithium metal with 30 nm thick coating Li_3PO_4 thin film demonstrates the best cycling performance and smallest electrochemical polarization. Besides acting as a protecting layer to prevent the reaction between lithium foil and electrolytes, its amorphous nature with homogeneous current density distribution on its surface along with tunnel effect is believed to be powerful for depressing lithium dendrite growth.

2. Experimental

2.1. Preparation of Li_3PO_4 thin film coated lithium metal foils

The Li metal foil (200 μm in thickness) was purchased from Tianqi Li Corporation, and was used as received. Li_3PO_4 thin film was deposited on Li metal foil by radio-frequency (RF) magnetron sputtering using a commercial Li_3PO_4 target (99.99%). The sputtering was performed at a fixed power (160 W) under 1.0 Pa argon pressure and target-to-substrate distance was fixed to be 5 cm. During sputtering, the substrate was rotated to guarantee a uniform coating. The sputtering time was changed from 5 min to 30 min to tune the coating thickness. The average sputtering rate is estimated to be 2 nm/min by measuring the thickness of the Li_3PO_4 film additionally deposited on silicon wafers. The surface-coated Li electrodes are denoted as Li/Li_3PO_4-x nm (x represents the thickness of Li_3PO_4 thin film) in the following text. For Li_3PO_4 conductivity measurement, we designed a Cu/Li_3PO_4/Cu structure on the quartz glass and the Cu film and Li_3PO_4 film with the thickness 200 nm and 1 μm, respectively. Our sputtering chamber is connected with the glove box. The samples can be directly transferred into the glove box without exposure to the air.

2.2. Material characterizations and electrochemical tests

The morphology was characterized by field-emission scanning electron microscope (FE-SEM, Hitachi, S3400N) and the crystalline of Li_3PO_4 film was investigated by transmission electron microscope (TEM, JEOL JEM-2100). And the compositions were analyzed with an energy dispersive X-ray spectroscopy (EDS, Oxford INCA PentaFET-X3).

As for the Li-S battery, the carbon/sulfur (C/S) composite was prepared by heating a mixture of Ketjen Black and sublimed sulfur powder (99.5%, Aladdin) in the weight ratio of 1:2 at 155 °C for 12 h. Subsequently, the C/S composite (80 wt%), acetylene black (10 wt%), and polyvinylidene fluoride (binder, 10 wt%) were mixed with *N*-methylpyrrolidone on a piece of Al foil. Afterward, the sulfur cathode was dried at 60 °C in vacuum for 12 h. Finally, the cathode was punched into a disk ($\Phi = 10$ mm) for assembling Li-S cells. Li-Li symmetric cells were assembled in a glove-box filled with an argon atmosphere. 1 M $LiPF_6$ dissolved in a mixture of ethylene carbonate (EC), diethyl carbonate (DEC), dimethyl carbonate (DMC) (1:1:1, v/v) was used as the liquid electrolyte. The separators (Celgard2400) were dried in vacuum overnight at 50 °C. The Li-S cells were assembled by the same way except with sulfur electrode as the working electrode. 1 M lithium bis(trifluoromethanesulphonyl) imide (LiTFSI) dissolved in 1,2-dimethoxyethane (DME) and 1,3-dioxolane (DOL) (1:1 by volume) (Zhangjiagang Guotai-Huarong New Chemical Materials Co. Ltd.) was used as electrolyte for Li-S batteries. The galvanostatic charge/discharge tests were performed using a CT2001A cell test instrument (LAND Electronic Co. Ltd.) at room temperature. The current density of Li-Li symmetric cells is 0.5 mA/cm^2 for each step with firstly discharge time of 0.5 h. The Li-S cells were tested in a voltage range of 1.7–2.8 V (*vs.* Li/Li$^+$) at a rate of 0.5 *C* (1 *C* = 1675 mA/g). Electrochemical impedance

spectroscopy (EIS) measurements were tested using an electrochemical workstation (CHI660B) in the frequency range from 100 kHz to 1 mHz with a perturbation amplitude of 10 mV. The DC polarization tests were carried out using a Solartron SI1287 equipment with 300 mV polarization voltage.

3. Results and discussion

The morphology of lithium metal with and without Li_3PO_4 coating was investigated by SEM, as shown in Fig. 1a–b. It can be seen that the surface of the pristine Li electrode is overall smooth with several bulges. After sputtering 20 min, a glassy layer Li_3PO_4 with 30 nm thickness is conformal and homogeneously coated on the Li foil. It is known that films obtained via magnetron sputtering at room temperature normally produce glassy amorphous phases. This is consistent with our previous study of Li_3PO_4 layer on $LiCoO_2$ prepared under similar condition that has no diffraction peak in XRD patterns [36]. From our TEM study, the obtained Li_3PO_4 has amorphous nature which shows no diffraction ring in the SAED pattern, as shown in Fig. 1c. In order to investigate the transport

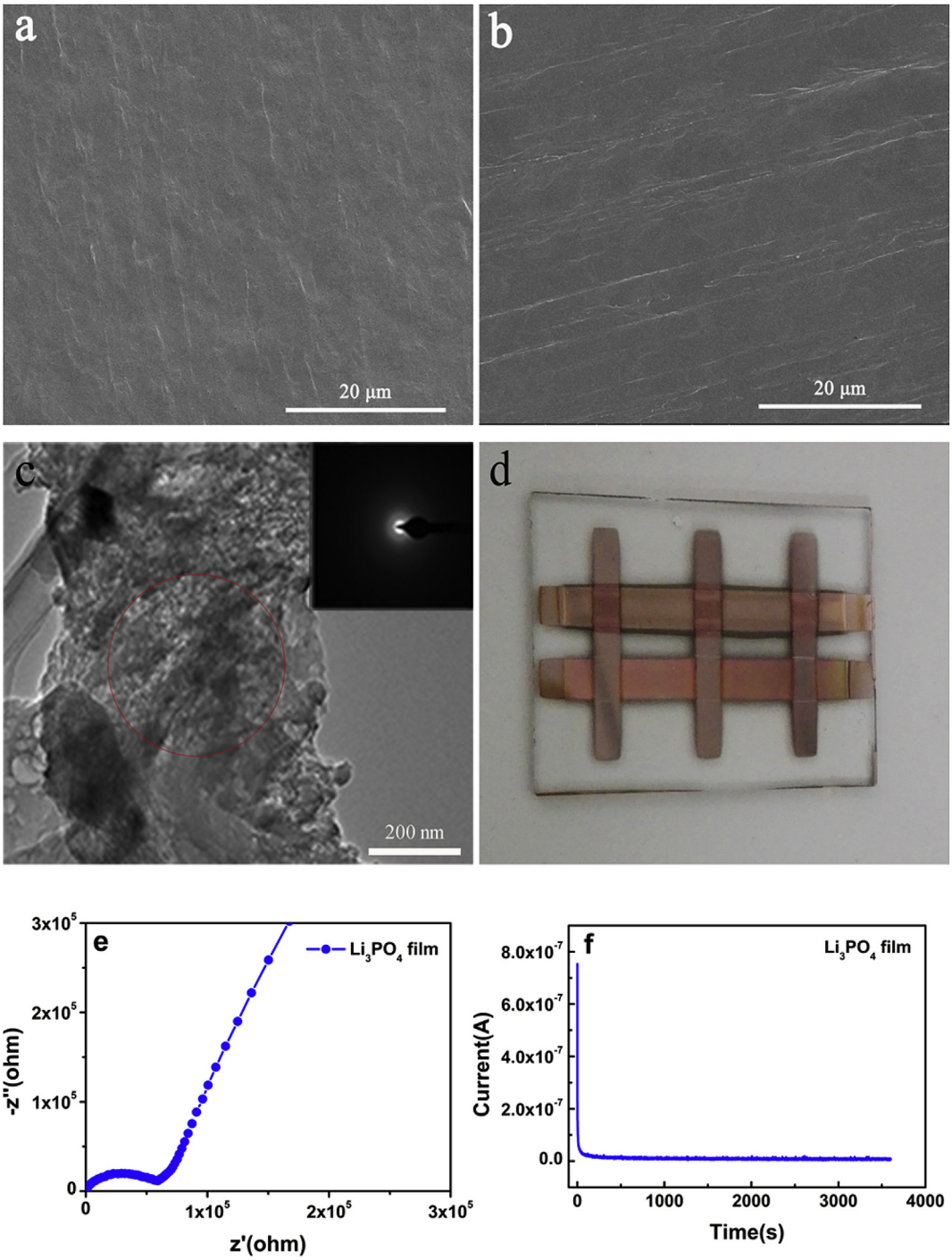

Fig. 1. Surface SEM morphologies of (a) pristine Li electrode, (b) surface modified Li electrode with 30 nm-thickness Li_3PO_4 coating, (c) TEM morphologies and SAED pattern of Li_3PO_4 film, (d) the image of Cu/Li_3PO_4/Cu structure, (e) Nyquist (complex impedance) plots for Li_3PO_4 film, (f) DC polarization current curves of Li_3PO_4 film.

properties of Li_3PO_4, we made a sandwich structure Cu/Li_3PO_4/Cu electrode and conducted EIS and DC polarization measurements (Fig. 1d–f). The electronic conductivity and ionic conductivity are 1.4×10^{-10} S/cm and 2.8×10^{-8} S/cm, respectively, a comparable magnitude with 3.3×10^{-7} S/cm of excimer laser deposited amorphous Li_3PO_4 thin film [37].

As reported by Aurbach et al., Li is thermodynamically unstable in organic solvents [9,38]. Therefore, the stability of interface is critical for Li metal anodes [22]. To investigate the stability of interface about Li metal electrode, EIS tests were carried out on the symmetric Li-Li cells at open circuit voltage. Fig. 2a–b displays the time dependence of the AC impedance spectra of symmetric Li-Li cells with/without Li_3PO_4 coating in commercial organic electrolytes. To have an overall understanding, we simply take the semicircle at high frequency in the spectra to represent an overall resistance R including both charge-transfer resistance (R_{ct}) and solid electrolyte interface layer (R_{SEI}). Initially, the R of the pristine Li-Li symmetric cell is smaller than that of the cell assembled with Li/Li_3PO_4-30 nm electrode, owing to the presence of Li_3PO_4 coating layer on the surface of Li metal electrode. With the increase of time, the R of the pristine Li cell increased continuously, which attributes to the gradual growth of SEI layer due to the reaction between Li metal electrode and electrolyte. Nevertheless, the R of Li/Li_3PO_4-30 nm cell reaches stable after 12 h indicating that the 30 nm Li_3PO_4 coating layer on the surface of Li metal electrode effectively isolate the Li electrode and organic electrolytes thus to prevent the side reaction. To evaluate the compactness of the Li_3PO_4 film by sputter-coating on Li metal, the pristine Li foil and the Li/Li_3PO_4-30 nm foil were also placed in ambient air for 60 min. The humidity is 80% and the temperature is about 25 °C for the exposure to air experiment. As shown in Fig. 2c–d, the pristine Li sheet tarnished and became black within few seconds while the modified Li electrode still kept the silvery white after one minute as the Li metal is extremely active to react with O_2, N_2 and H_2O in air atmosphere [39]. The color change of Li foil indicates that new compositions formed on the surface of Li metal, such as lithium nitride (Li_3N), lithium oxide (Li_2O), lithium hydroxide (LiOH), lithium carbonate (Li_2CO_3). Therefore, the Li_3PO_4 film deposited on the surface of Li foil by magnetron sputtering is conformal to lithium metal.

We investigate the electrochemical behavior of plating/stripping and cycling stability of Li_3PO_4-coated lithium metal anodes. Fig. 3a–e shows the voltage-time profiles of the symmetric Li-Li cells under galvanostatic charge-discharge current density of 0.5 mA/cm^2. Electrodes with different coating thickness (0 nm, 10 nm, 30 nm, 60 nm) demonstrate similar results: at the very beginning electrochemical polarizations are observed followed by long periods of stable, and finally all the cells occur failures after different cycles. The pristine Li electrode cell arises a short circuit after 400 h possibly owning to electrolyte decomposition and Li dendrites growth. Whereas, the Li/Li_3PO_4-10 nm electrode, Li/Li_3PO_4-30 nm electrode, and Li/Li_3PO_4-60 nm electrode occur short circuits after 650 h, 900 h (corresponding to 450 cycles), and 570 h, respectively. It is clear that the modified Li electrode with 30 nm Li_3PO_4 possesses the longest cycle life. As the deposited Li_3PO_4 thin film has a low electronic conductivity (10^{-10} S/cm) and ionic conductivity (10^{-8} S/cm), lithium metal with 60 nm Li_3PO_4 coating could cause a kinetic limitation for Li^+ transport, which leads a large electrochemical polarization attributing a worse performance compared with the Li/Li_3PO_4-30 nm electrode. Meanwhile, the same trend for the voltage-time curves is observed at a higher current density of 1 mA/cm^2 for 1 h in the pristine Li electrode and Li/Li_3PO_4-30 nm electrode. This Li/Li_3PO_4-30 nm electrode has a comparable life time than the one obtained by Kazyak et al. using 2 nm thick Al_2O_3 layers coated lithium metals via atomic layer deposition [30] and the one by Yang and coauthors introducing 3D Cu current collectors to have 120 cycles under current density of 0.2 mA/cm^2 [14].

To elucidate the interfacial stability of modified Li electrodes, EIS measurements are applied to the symmetric batteries after different cycles as shown in Fig. 4. The equivalent circuit (Fig. 4a, inset) as similar in our previous work was used to fit these impedance spectra using Zview software and the R_s, R_f, and R_{ct} represent the internal resistance of the cell, surface layer resistance, and charge-transfer resistance, respectively [36,40,41]. The fitting

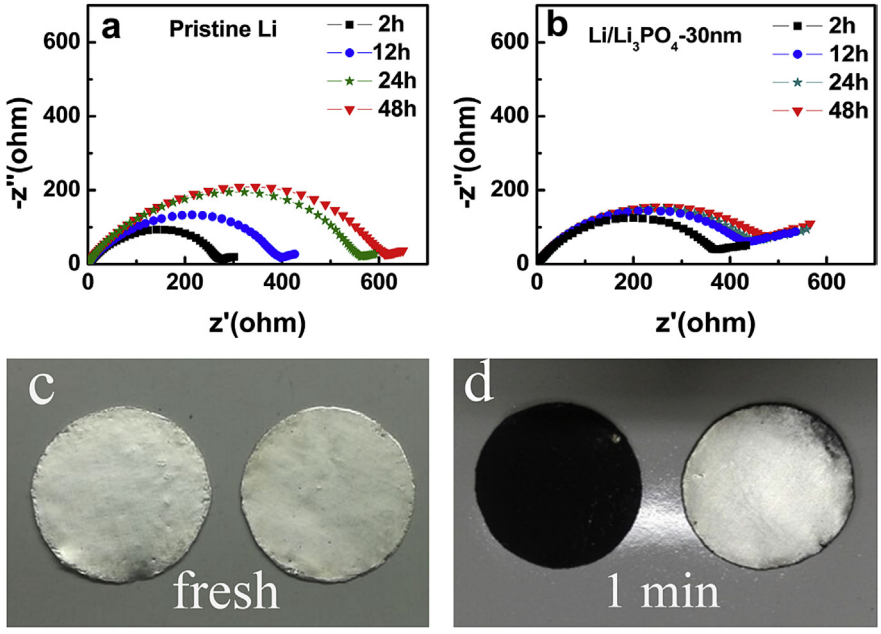

Fig. 2. AC impedance spectra of the symmetric Li-Li cells with (a) pristine Li and (b) Li/Li_3PO_4-30 nm electrodes as function of storage time at room temperature. Photographic images showing the corrosion of Li metal electrodes exposed to the air with different elapse time of (c) fresh and (d) 1 min. The left disc of image is pristine Li and the right disc is Li/Li_3PO_4-30 nm.

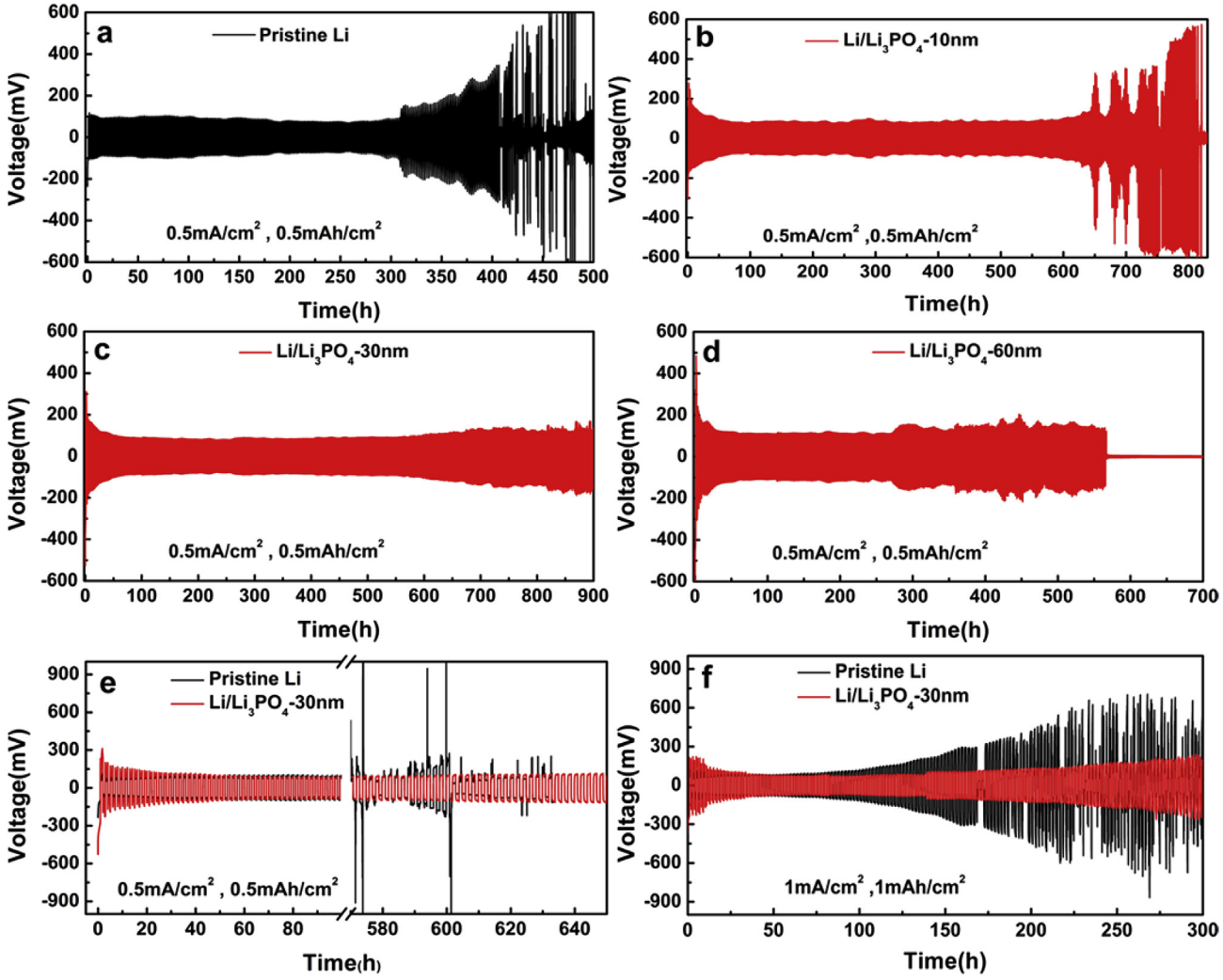

Fig. 3. Galvanostatic cycling of a symmetric Li-Li cells with different electrodes (a) pristine Li, (b) Li/Li_3PO_4-10 nm, (c) Li/Li_3PO_4-30 nm, (d) Li/Li_3PO_4-60 nm. The current density was fixed at 0.5 mA/cm^2 with a discharge/charge capacity of 0.5 mAh/cm^2. (e) Enlarged voltage profiles of the symmetric Li-Li cells with pristine Li electrode and Li/Li_3PO_4-30 nm electrode. (f) Comparison of voltage profiles of the symmetric Li-Li cells with pristine Li electrode and Li/Li_3PO_4-30 nm electrode in 1 mA/cm^2 with a discharge/charge capacity of 1 mAh/cm^2.

results are summarized in Table 1. The overall resistance is a sum of the R_s, R_f and R_{ct}. It is found that the overall resistance for pristine Li and Li/Li_3PO_4- 30 nm are 203 Ω and 378 Ω, respectively. The Li_3PO_4 coated lithium has a higher resistance due to interfacial resistance of the physical coating of Li_3PO_4. After stripping and plating processes in the first several cycles, the interface reacts sufficiently with electrolytes so that both of the pristine and modified electrodes have smaller resistance, which is also called an activation process [30]. While, in the subsequent cycles, the impedance of pristine Li electrode increased gradually from 51 Ω (at 50th cycle) to 240 Ω (at 200th cycle) as explained by the formation of unstable and insulator species between lithium and electrolytes which is evidenced by the clear increase of R_f. In contrast, the Li/Li_3PO_4-30 nm electrode impedance value is almost invariant from 81 Ω (at 50th cycle) to 87 Ω (at 200th cycle). This phenomenon strongly demonstrates that interfacial stability of Li_3PO_4-treated Li electrode is much better than pristine Li electrode, which is very important for the long term cycling of lithium metal electrodes.

The symmetric Li-Li cells were dissembled and SEM was imported to view the morphologies of Li electrodes after charge/discharge cycling. Fig. 5 displays the cross-section images, surface morphologies images, and surface EDS spectra of pristine Li and Li/Li_3PO_4-30 nm electrodes after 100 cycles at current density of 0.5 mA/cm^2 with a discharge/charge capacity of 0.5 mAh/cm^2. As can be seen, the cycled Li metal exhibits rough and porous surface structure with a thickness of 70 μm of "dead Li" layer and SEI layer from cross section image. And the surface of pristine Li electrode shows mass dendritic Li under higher magnifications (Fig. 5 b–c). The main reason of dendritic Li growth is the inhomogeneous Li deposition. The gradual thickening "dead Li" layer and SEI layer are attributed to plenty of Li dendrites disconnecting from bulk Li and a large amount of SEI components produced on the surface of Li electrode in the repeated breakage/repair of the SEI process due to the reaction between active Li and organic electrolyte. Regarding the Li/Li_3PO_4-30 nm electrode, it displays flat and compact surface with extremely thin SEI layer. The Li_3PO_4 thin film still exists on the surface of Li metal after 100 cycles as evidenced by our EDS spectra (Fig. 5h). This consequently proves that the treated Li metal electrode with 30 nm amorphous Li_3PO_4 layer can sufficiently and effectively restrain the lithium dendrite growth, which is suspected to have correlation with the amorphous and chemical stable properties of Li_3PO_4 thin films.

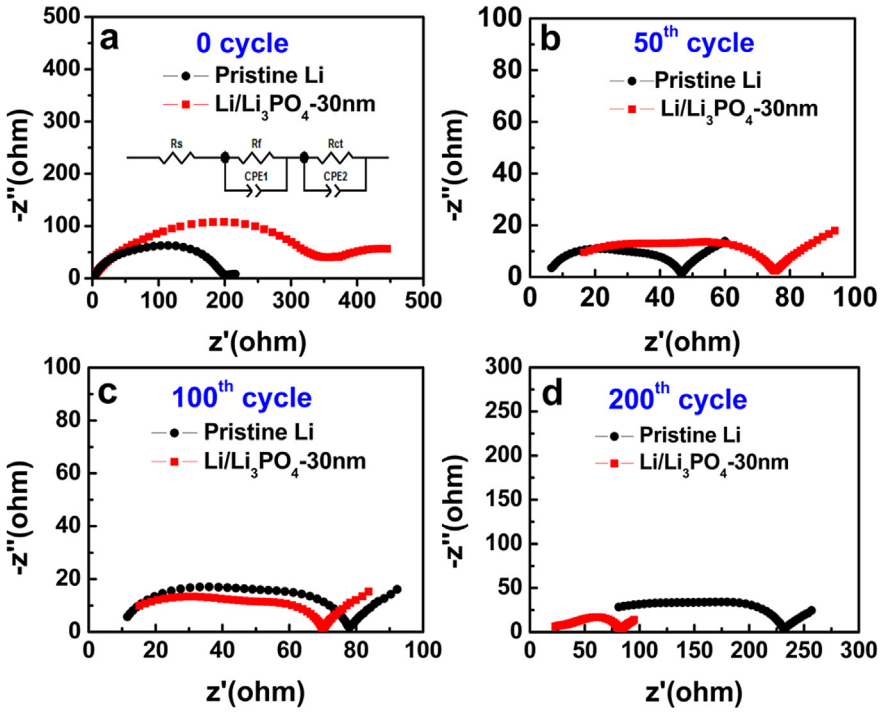

Fig. 4. Electrochemical impedance spectra of pristine and 30 nm Li_3PO_4 -modified electrodes in symmetric Li-Li cells was obtained at open circuit voltage after rest for 20 h when the charge-discharge process under current density of 0.5 mA/cm^2 was completed. (a) fresh cell state, (b) after 50 cycles, (c) after 100 cycles, (d) after 200 cycles.

Table 1
Fitting parameters of EIS for the bare Li metal and the Li_3PO_4 modified Li metal.

Cycle	Pristine Li				Li/Li_3PO_4-30 nm			
	R_s	R_f	R_{ct}	$R_{overall}$	R_s	R_f	R_{ct}	$R_{overall}$
0	3.3	154.7	44.7	202.7	2.5	363.4	11.6	377.5
50th	6.5	15.2	28.9	50.6	16.4	51.2	13.6	81.2
100th	11.6	48.0	22.1	81.7	15.2	62.9	17.7	95.8
200th	81.3	122.9	35.4	239.6	22.2	57.8	6.9	86.9

To better elaborate the impact of Li_3PO_4 on the lithium metal foil, we make a schematic illustration as shown in Fig. 6. Firstly, the as-prepared homogeneous chemical inert Li_3PO_4 film is a good physical shield to prevent the chemical reaction between lithium metal and the electrolyte, thus to avoid the yield of the unstable SEI. In this part, the Li_3PO_4 acts as an artificial stable SEI role that can avoid eating lithium and continuously increase of charge-transfer resistance, which brings in low coulombic efficiency and

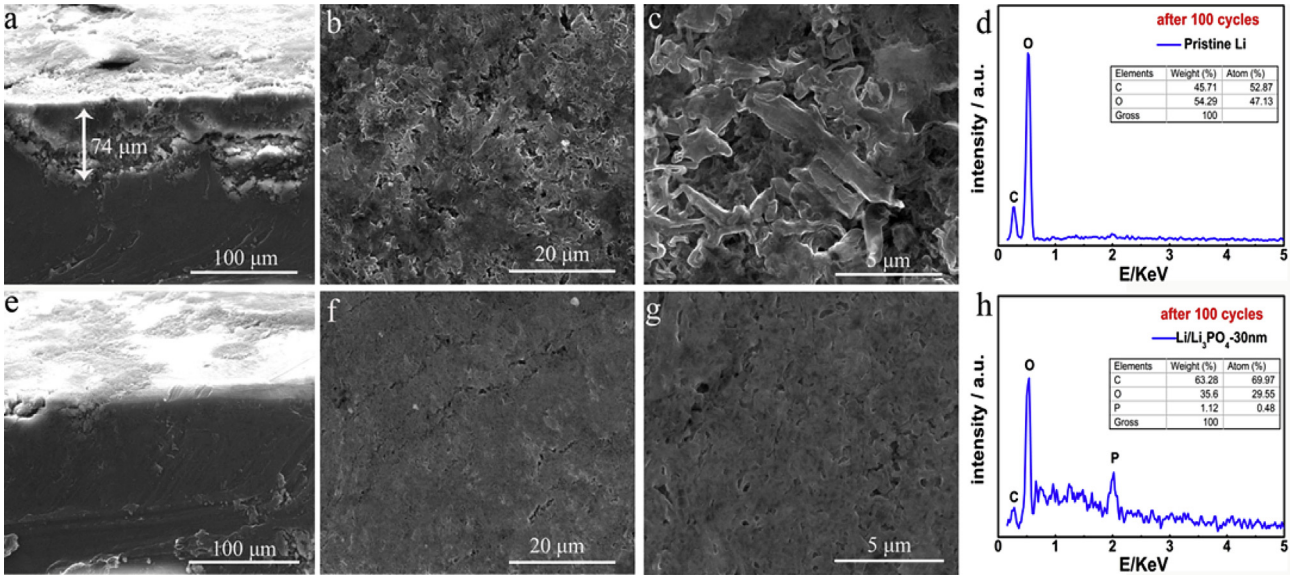

Fig. 5. (a) Cross-section SEM image, (b) and (c) surface SEM images, surface EDS spectra (d) of the pristine Li metal electrode after 100 cycles, (e) Cross-section SEM image, (f) and (g) surface SEM images, and (h) surface EDS spectra of the Li/Li_3PO_4-30 nm electrode after 100 cycles.

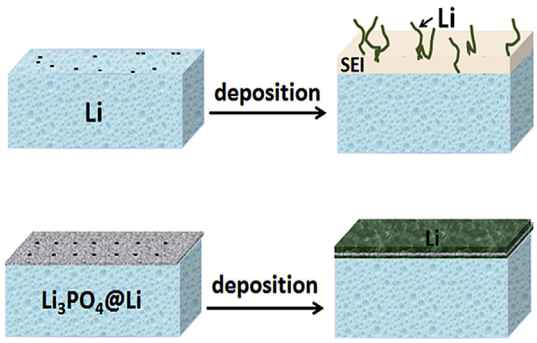

Fig. 6. Schematic illustrations for the effect of Li_3PO_4 coating on lithium metal foils.

higher electrochemical polarization. And this is supported by our cycling performance test (Fig. 3) and EIS spectra study shown in Fig. 4. Secondly, we believe that the amorphous nano-thickness film provides a homogenous current density distribution instead of the anisotropic current distribution from the crystal metallic lithium. Accumulated current density favors fast lithium nucleation and growth, easily producing lithium dendrite in islands form instead of layer-by-layer growth mechanism. Since the ionic conductivity in Li_3PO_4 is small (2.8×10^{-8} S/cm) and the charge-discharge current are pretty large 0.5–1 mA/cm^2, the lithium ions are easily accumulated on the surface of Li_3PO_4 rather than pass through it. Meanwhile, the electrons from the current collector side crossover the nano thick Li_3PO_4 film owning to tunnel effect to neutron Li^+ for lithium metal deposition. Regarding this, the amorphous nature of Li_3PO_4 without anisotropy is of prime importance. And it is supported by the SEM evidence (Fig. 5) that the lithium is deposited onto the surface of Li_3PO_4 without dendrite formation.

It is known to us that the lithium sulfur and lithium oxygen batteries are flagships for the applications of lithium metal. Hence, we apply the Li_3PO_4 modified Li metal as an anode in the Li-S battery to check its property behavior, as displayed in Fig. 7. Note that this is whole cell performance, a combination contribution of both lithium anode and sulfur cathode, rather than a simply cathode sulfur contribution. Fig. 7a depicts the galvanostatic charge-discharge curves for Li-S batteries. A little smaller than the theoretical capacity 1675 mAh/g of Li-S, the initial discharge capacities for both cells are about 1000 mAh/g, which is believed due to polarizations and can be partly improved by optimizing the electrode preparation and decreasing current density. The Li_3PO_4 treated Li-S cell has a larger polarization in the initial cycle than the pristine one because of the difficult transportation of lithium ions in Li_3PO_4 thin film leading a concentration polarization. Luckily, with activation process and stable property to electrolyte, the Li_3PO_4-treated cell has a larger capacity and lower polarization than the bare one as evidenced in the 200 cycles. Fig. 7b shows the cycle performance and coulombic efficiency of Li–S cells assembled with different Li anodes at 0.5 *C*. The discharge capacity of the Li-S cell with 30 nm Li_3PO_4 modified Li metal electrode remains 486 mAh/g at 0.5 *C* with capacity retention 52% after 200 cycles, while the Li-S cell with pristine Li metal electrode displays a discharge capacity of 247 mAh/g at 0.5 *C* with a capacity retention only 28% after 200 cycles. The average coulombic efficiency of Li-S cells with a Li_3PO_4 protected Li electrode is as high as 89%, which is much superior to the Li-S cells with pristine Li electrode with 84%. In words, the improvement of lithium metal anode parts can concomitantly improve the whole performance of the cell.

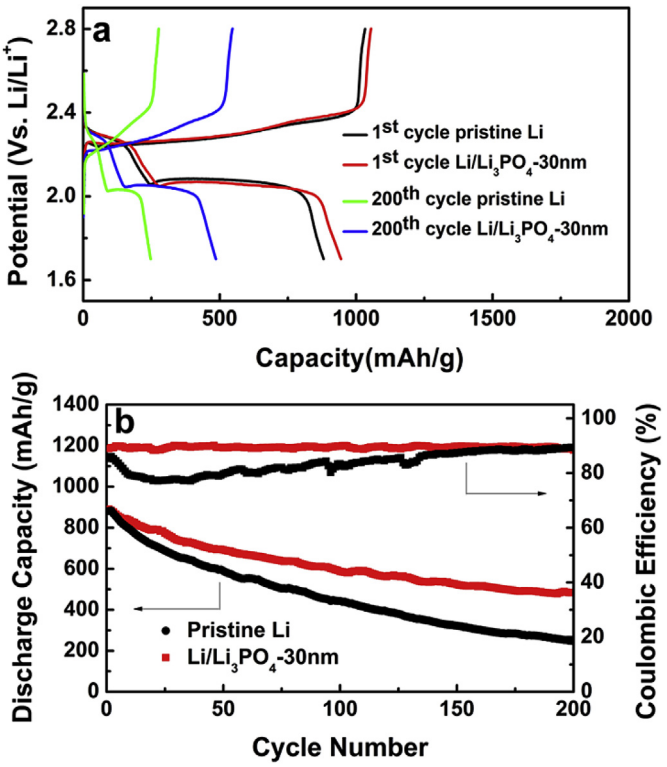

Fig. 7. (a) The initial and 200th cycling charge–discharge profiles of Li-S cells with different Li anodes at 0.5 *C*. (b) The cycle performance and coulombic efficiencies of Li–S cells assembled with different Li anodes at 0.5 *C*.

4. Conclusions

In summary, amorphous Li_3PO_4 thin films with different nanometer thickness are homogeneously coated on the lithium metal anodes via a facile and economic method, namely magnetron sputtering. We have evidenced that the 30 nm thick thin film Li_3PO_4 coated Li metal anodes presents a long cycling life and low electrochemical polarizations. It is found that Li_3PO_4 not only acts a role in stabilizing the interface between lithium metals and electrolytes, but more importantly, gives a homogeneous current density distribution for uniform lithium deposition instead of dendrites thanks to Li_3PO_4 isotropy amorphous nature. The idea to modify current density distribution using nanometer thickness amorphous films describes an unprecedented strategy to control the morphology of lithium deposition. These findings help us to elucidate the mechanistic growth of lithium dendrites and provide valuable insights into proper designing coating films to improve the properties of lithium metal batteries.

Acknowledgments

This work is supported by the National Science Foundation of China (51502032, 21673033, 11234013, 21473022), the Science and Technology Bureau of Sichuan Province of China (no.2015HH0033), and the Opening Project of State Key Laboratory of Polymer Materials Engineering (Sichuan University) (Grant No. Sklpme2016-4-23).

References

[1] C.X. Zu, H. Li, Energy Environ. Sci. 4 (2011) 2614–2624.
[2] F. Ding, W. Xu, G.L. Graff, J. Zhang, M.L. Sushko, X.L. Chen, Y.Y. Shao, M.H. Engelhard, Z.M. Nie, J. Xiao, X.J. Liu, P.V. Sushko, J. Liu, J.G. Zhang, J. Am.

Chem. Soc. 135 (2013) 4450–4456.
[3] X.Y. Dai, L.P. Wang, J. Xu, Y. Wang, A.J. Zhou, J.Z. Li, ACS Appl. Mater. interfaces 6 (2014) 15853–15859.
[4] J.J. Wang, X.L. Sun, Energy Environ. Sci. 5 (2012) 5163–5185.
[5] X.B. Meng, X.Q. Yang, X.L. Sun, Adv. Mater. 24 (2012) 3589–3615.
[6] Y.N. Zhou, M. Sina, N. Pereira, X.Q. Yu, G.G. Amatucci, X.Q. Yang, F. Cosandey, K.W. Nam, Adv. Funct. Mater. 25 (2015) 696–703.
[7] E. Baudrin, G. Sudant, D. Larcher, B. Dunn, J.M. Tarascon, Chem. Mater. 18 (2006) 4369–4374.
[8] H. Zhang, Q. Deng, C. Mou, Z. Huang, Y. Wang, A. Zhou, J. Li, J. Power Sources 239 (2013) 538–545.
[9] D. Aurbach, E. Zinigrad, Y. Cohen, H. Teller, Solid State Ionics 148 (2002) 405–416.
[10] D. Aurbach, J. Power Sources 89 (2000) 206–218.
[11] W. Li, H. Zheng, G. Chu, F. Luo, J. Zheng, D. Xiao, X. Li, L. Gu, H. Li, X. Wei, Q. Chen, L. Chen, Faraday Discuss. 176 (2014) 109–124.
[12] B.L. Mehdi, J. Qian, E. Nasybulin, C. Park, D.A. Welch, R. Faller, H. Mehta, W.A. Henderson, W. Xu, C.M. Wang, J.E. Evans, J. Liu, J.G. Zhang, K.T. Mueller, N.D. Browning, Nano Lett. 15 (2015) 2168–2173.
[13] C. Brissot, M. Rosso, J.N. Chazalviel, P. Baudry, S. Lascaud, Electrochim. Acta 43 (1998) 1569–1574.
[14] C.P. Yang, Y.X. Yin, S.F. Zhang, N.W. Li, Y.G. Guo, Nat. Commun. 6 (2015).
[15] J.F. Qian, W.A. Henderson, W. Xu, P. Bhattacharya, M. Engelhard, O. Borodin, J.G. Zhang, Nat. Commun. 6 (2015).
[16] J.S. Kim, D.W. Kim, H.T. Jung, J.W. Choi, Chem. Mater. 27 (2015) 2780–2787.
[17] W. Xu, J.L. Wang, F. Ding, X.L. Chen, E. Nasybutin, Y.H. Zhang, J.G. Zhang, Energy Environ. Sci. 7 (2014) 513–537.
[18] W.S. Jia, C. Fan, L.P. Wang, Q.J. Wang, M.J. Zhao, A.J. Zhou, J.Z. Li, ACS Appl. Mater. interfaces 8 (2016) 15399–15405.
[19] D. Aurbach, E. Pollak, R. Elazari, G. Salitra, C.S. Kelley, J. Affinito, J. Electrochem. Soc. 156 (2009) A694–A702.
[20] Y. Ito, A. Sakuda, T. Ohtomo, A. Hayashi, M. Tatsumisaga, Electrochemistry 82 (2014) 591–594.
[21] S.J. Lee, H.K. Balk, S.M. Lee, Electrochem. Commun. 5 (2003) 32–35.
[22] N.W. Li, Y.X. Yin, C.P. Yang, Y.G. Guo, Adv. Mater. 28 (2016) 1853–1858.
[23] Y.J. Zhang, X.Y. Liu, W.Q. Bai, H. Tang, S.J. Shi, X.L. Wang, C.D. Gu, J.P. Tu, J. Power Sources 266 (2014) 43–50.
[24] H. Lee, D.J. Lee, Y.J. Kim, J.K. Park, H.T. Kim, J. Power Sources 284 (2015) 103–108.
[25] G.Q. Ma, Z.Y. Wen, Q.S. Wang, C. Shen, J. Jin, X.W. Wu, J. Mater. Chem. A 2 (2014) 19355–19359.
[26] W. Luo, L.H. Zhou, K. Fu, Z. Yang, J.Y. Wan, M. Manno, Y.G. Yao, H.L. Zhu, B. Yang, L.B. Hu, Nano Lett. 15 (2015) 6149–6154.
[27] X.L. Zhang, W.K. Wang, A.B. Wang, Y.Q. Huang, K.G. Yuan, Z.B. Yu, J.Y. Qiu, Y.S. Yang, J. Mater. Chem. A 2 (2014) 11660–11665.
[28] H. Kim, J.T. Lee, D.C. Lee, M. Oschatz, W.I. Cho, S. Kaskel, G. Yushin, Electrochem. Commun. 36 (2013) 38–41.
[29] A.C. Kozen, C.F. Lin, A.J. Pearse, M.A. Schroeder, X.G. Han, L.B. Hu, S.B. Lee, G.W. Rubloff, M. Noked, Acs Nano 9 (2015) 5884–5892.
[30] E. Kazyak, K.N. Wood, N.P. Dasgupta, Chem. Mater. 27 (2015) 6457–6462.
[31] G.Y. Zheng, S.W. Lee, Z. Liang, H.W. Lee, K. Yan, H.B. Yao, H.T. Wang, W.Y. Li, S. Chu, Y. Cui, Nat. Nanotechnol. 9 (2014) 618–623.
[32] N.J. Dudney, J. Power Sources 89 (2000) 176–179.
[33] B. Wang, B.C. Chakoumakos, B.C. Sales, B.S. Kwak, J.B. Bates, J. Solid State Chem. 115 (1995) 313–323.
[34] P. Bai, J. Li, F.R. Brushett, M.Z. Bazant, Energy Environ. Sci. 9 (2016) 3221–3229.
[35] L. Chen, H.W. Zhang, L.Y. Liang, Z. Liu, Y. Qi, P. Lu, J. Chen, L.-Q. Chen, J. Power Sources 300 (2015) 376–385.
[36] A.J. Zhou, J. Xu, X.Y. Dai, B. Yang, Y.T. Lu, L.P. Wang, C. Fan, J.Z. Li, J. Power Sources 322 (2016) 10–16.
[37] N. Kuwata, N. Iwagami, Y. Tanji, Y. Matsuda, J. Kawamura, J. Electrochem. Soc. 157 (2010) A521–A527.
[38] Y.S. Cohen, Y. Cohen, D. Aurbach, J. Phys. Chem. B 104 (2000) 12282–12291.
[39] S.M. Choi, I.S. Kang, Y.K. Sun, J.H. Song, S.M. Chung, D.W. Kim, J. Power Sources 244 (2013) 363–368.
[40] X.Y. Dai, A.J. Zhou, J. Xu, Y.T. Lu, L.P. Wang, C. Fan, J.Z. Li, J. Phys. Chem. C 120 (2016) 422–430.
[41] X.Y. Dai, A.J. Zhou, J. Xu, B. Yang, L.P. Wang, J.Z. Li, J. Power Sources 298 (2015) 114–122.